Characterization of Gold Nanoparticles Modified with Single-Stranded DNA Using Analytical Ultracentrifugation and Dynamic Light Scattering

ARTICLE *in* LANGMUIR · AUGUST 2010

Impact Factor: 4.46 · DOI: 10.1021/la100761f · Source: PubMed

5 AUTHORS, INCLUDING:

Tae Joon Cho
National Institute of Standards and Technol…
38 PUBLICATIONS **781** CITATIONS
SEE PROFILE

Vincent A. Hackley
National Institute of Standards and Technol…
111 PUBLICATIONS **2,094** CITATIONS
SEE PROFILE

Langmuir
Article

pubs.acs.org/Langmuir

Characterization of Gold Nanoparticles Modified with Single-Stranded DNA Using Analytical Ultracentrifugation and Dynamic Light Scattering

James B. Falabella,* Tae Joon Cho, Dean C. Ripple, Vincent A. Hackley, and Michael J. Tarlov

National Institute of Standards and Technology, Gaithersburg, Maryland 20899

Received February 21, 2010. Revised Manuscript Received June 6, 2010

We report the characterization of gold nanoparticles modified with thiol-terminated single stranded DNA (ssDNA) using analytical ultracentrifugation. Dynamic light scattering was used to measure the diameter of bare and ssDNA modified gold nanoparticles to corroborate the predictions of our models. Sedimentation coefficients of nominally 10 and 20 nm diameter gold nanoparticles modified with thiol-terminated thymidine homo-oligonucleotides, 5−30 bases in length, were determined with analytical ultracentrifugation. The sedimentation coefficients of gold nanoparticles modified with ssDNA were found to decrease with increasing coverage of ssDNA and increasing length of ssDNA. The sedimentation coefficients of ssDNA modified gold particles were most closely predicted when the strands were modeled as fully extended chains (FEC). Apparent particle densities of bare gold nanoparticles calculated from measured sedimentation coefficients decreased significantly below that of bulk gold with decreasing size of nanoparticles. This finding suggests that hydration layer effects are an important factor in the sedimentation behavior for both bare and short ssDNA chain modified gold particles.

Introduction

Biologically modified nanomaterials are being intensely studied and developed for a variety of biomedical applications. These materials are being considered for use as therapeutic agents, vehicles for targeted drug delivery, and diagnostic probes.[1−4] In therapeutic applications, these materials are expected to receive intense regulatory scrutiny in order to be approved for use in human subjects. Any nanoparticle-based therapeutic will undergo rigorous characterization using an arsenal of orthogonal methods to assess the critical physical, chemical, and biological attributes that contribute to its efficacy and safety. Among these attributes, particle size distribution and biomolecular surface coverage will likely figure prominently and robust analytical methods will be needed for their assessment.

If a nanoparticle-based therapeutic is coated with biomolecules, the molecular surface loading of each batch should be monitored to detect any significant variation that might affect drug efficacy or safety. The conformation of the molecules at the surface of a biologically modified nanoparticle will also be important because a change in the molecular surface configuration may reduce the accessibility of active sites or possibly lead to aggregation of the particles. The presence of aggregates of particles may be of particular concern because of the possibility of these aggregates being immunogenic, i.e., causing an immune reaction in patients that leads to neutralization of the drug, similar to what has been observed for aggregated protein therapeutics and vaccines.[5,6] Ensuring a proper size distribution within a batch of biologically modified nanomaterials may also affect drug efficacy and safety because many of these therapies will likely exploit the selectivity in delivery afforded by the relatively larger openings in the walls of blood vessels in the cancerous tissue.[7]

There are several well-established methods for sizing nanomaterials that can also be used to detect their potential aggregation and provide information concerning their surface modification. Among the most widespread are size exclusion chromatography (SEC),[8,9] asymmetric field flow fractionation (AFFF),[10,11] dynamic light scattering (DLS),[12,13] and analytical ultracentrifugation (AUC).[10,14] Size distributions from DLS alone are nontrivial to obtain without prior knowledge of whether aggregation is occurring.[10] If the particles differ in hydrodynamic diameter by less than several fold, one must employ AFFF to pre classify particles before performing DLS. The membrane unit for performing AFFF dilutes the sample in the process of segregating the particles of different size, which can decrease the measured concentration of aggregates if the particles are reversibly associated. Krueger et al.[9] recently employed SEC to separate polystyrene stabilized nanoparticles of Au and CdSe in toluene. SEC often requires sample dilution, which can also alter aggregate distributions, and the interaction of the material with the column matrix may further perturb aggregates.

*To whom correspondence should be addressed.

(1) Talley, C. E.; Jackson, J. B.; Oubre, C.; Grady, N. K.; Hollars, C. W.; Lane, S. M.; Huser, T. R.; Nordlander, P.; Halas, N. J. *Nano Lett.* **2005**, *5*, 1569–1574.
(2) Corrigan, T. D.; Guo, S.; Phaneuf, R. J.; Szmacinski, H. *J. Fluoresc.* **2005**, *15*, 777–784.
(3) Corrigan, T. D.; Guo, S.-H.; Szmacinski, H.; Phaneuf, R. J. *Appl. Phys. Lett.* **2006**, *88*, 101112.
(4) Patra, C. R.; Bhattacharya, R.; Wang, E.; Katarya, A.; Lau, J. S.; Dutta, S.; Muders, M.; Wang, A.; Buhrow, S. A.; Safgren, S. L.; Yaszemski, M. J.; Reid, J. M.; Ames, M. M.; Mukherjee, P.; Mukhopadhyay, D. *Cancer Res.* **2008**, *68*, 1970–1978.
(5) Cedervall, T.; Lynch, I.; Lindman, S.; Berggard, T.; Thulin, E.; Nilsson, H.; Dawson, K. A.; Linse, S. *Proc. Natl. Acad. Sci. U.S.A.* **2007**, *104*, 2050–2055.
(6) Clausi, A. L.; Morin, A.; Carpenter, J. F.; Randolph, T. W. *J. Pharm. Sci.* **2009**, *98* (1), 114-121.
(7) Balogh, L.; Nigavekar, S. S.; Nair, B. M.; Lesniak, W.; Zhang, C.; Sung, L. Y.; Kariapper, M. S. T.; El-Jawahri, A.; Llanes, M.; Bolton, B.; Mamou, F.; Tan, W.; Hutson, A.; Minc, L.; Khan, M. K. *Nanomedicine* **2007**, *3*, 281–296.
(8) Krueger, K. M.; Al-Somali, A. M.; Mejia, M.; Colvin, V. L. *Nanotechnology* **2007**, *18*, 475709.
(9) Krueger, K. M., Al-Somali, A. M., Colvin, V. L. *Abstracts of papers*, 231st ACS National Meeting, Atlanta, GA; American Chemical Society: Washington DC, 2006; Abstract INOR-705.
(10) Liu, J.; Andya, J. D.; Shire, S. J. *AAPS J.* **2006**, *8*, E580–E589.
(11) Fraunhofer, W.; Winter, G. *Eur. J Pharm. Biopharm.* **2004**, *58*, 369–383.
(12) Bootz, A.; Vogel, V.; Schubert, D.; Kreuter, J. *Eur. J Pharm. Biopharm.* **2004**, *57*, 369–375.
(13) Millard, M. M.; Wolf, W. J.; Dintzis, F. R.; Willett, J. L. *Carbohydr. Polym.* **1999**, *39*, 315–320.
(14) Cole, J. L.; Lary, J. W.; Moody, T. P.; Laue, T. M. Analytical Ultracentrifugation: Sedimentation Velocity and Sedimentation Equilibrium. In *Methods in Cell Biology: Biophysical Tools for Biologists, Vol. One: In Vitro Techniques*; Correia, J. J., Detrich, H. W., Eds.; Academic Press: Boston, 2008; pp 143−179; Vol. *84*.

In contrast, analytical ultracentrifugation can examine samples over a wide range of solution conditions and concentrations and detect low levels of aggregated protein therapeutics that are difficult to detect with SEC. With subnanometer resolution,[15] AUC can often classify samples when other analytical methods fail to detect any difference in particle size or molecular surface coverage. Recently, nanoparticles of CdS,[16] CdSe,[16] and TiO_2[17] less than 20 nm in diameter were characterized with AUC and differences in sedimentation coefficients were attributed to varying surface texture of the nanoparticles. Mächtle et al.[18] also demonstrated the impressive range of particle sizes that can be measured with AUC by implementing a rotor speed gradient program to classify polystyrene spheres ranging from 20 to 2000 nm in diameter. AUC of biologically modified nanomaterials was recently reported by Calabretta et al.[19] and Jamison et al.[20] where they examined the formation of DNA−LacI protein complexes on the surface of 10 nm gold nanoparticles.[21,22] Their study showed that AUC could discern between LacI-modified gold nanoparticles with and without bound DNA. Although these recent investigations demonstrate the ability of AUC to distinguish between nanoparticles of different size and nanoparticles modified with biological molecules, there have been no AUC studies reported that have systematically examined the surface loading or length of biopolymers tethered to nanoparticles, such as single-stranded DNA (ssDNA) oligomers. To fill this gap, we report here the use of AUC to determine sedimentation coefficients of gold nanoparticles nominally 10 and 20 nm in diameter that are modified with thiol-terminated single-stranded thymine homo-oligomers from 5 to 30 bases in length. We compare the sedimentation coefficients determined using AUC for these materials with models that provide insight into the conformation of molecules at the particle surface.

Experimental Section

Chemicals. The nominally 10 nm diameter gold nanoparticles used in this study were National Institute of Standards and Technology (NIST) Reference Material (RM) 8011.[23] Other NIST reference materials used in this study are nominal (30 and 60) nm diameter gold nanoparticles (NIST RM 8012[24] and 8013[25]). This NIST reference material consists of citrate-stabilized gold nanoparticles suspended in water. The dimensions of these nanoparticles were measured by NIST using six independent methods—atomic force microscopy (AFM), transmission electron microscopy (TEM), scanning electron microscopy (SEM), electro spray-differential mobility analysis (ES-DMA), dynamic light scattering (DLS), and small-angle X-ray scattering (SAXS)—and these results are reported in the NIST Reports of Investigation. The nominally 5 and 20 nm diameter gold nanoparticles were purchased from Ted Pella (Redding, CA) and sized using ES-DMA in our laboratory according to the method of Pease et al.[26] The nanoparticles purchased from Ted Pella are electron microscopy grade with nominal particle concentrations of 5×10^{13} particles·mL^{-1} (5 nm diameter) and 7×10^{11} particles·mL^{-1} (20 nm diameter). When the number concentration is converted to a mass concentration treating the nanoparticles as spheres with the nominal diameters and number concentrations published on the supplier's Web site, the 5 nm gold particles are at a 0.63 mg·mL^{-1} concentration the 20 nm gold particles are at a 0.56 mg·mL^{-1} concentration. Thymidine homo-oligomers were purchased from Integrated DNA Technologies (Coral, IA) with a 3′ dithiol modification of the general formula $HO(CH_2)_3-S-S-(CH_2)_3-T_x$ (where subscript x is the number of bases which varies from 5 to 30) were used for all ssDNA−gold conjugates. NaCl (99.999% pure) and $MgCl_2$ were purchased from Aldrich (Milwaukee, WI) and used as received. Thymidine homo-oligomers in four different lengths including 5, 10, 20, and 30 bases were purchased to examine the effect of increasing ssDNA strand length. Ultra pure 18 MΩ·cm water from a Barnstead Nanopure UV water purifier (Beverly, MA) was used to prepare solutions for all experiments.

Procedure for Preparing Gold Nanoparticle−ssDNA Homo-Oligomer Conjugates. Thiolated thymidine homo-oligomers were first dissolved in deionized water to a concentration of 200 μmol·L^{-1}. To prepare the ssDNA−gold conjugates 6 μL of ssDNA stock solution was added to 100 μL of gold nanoparticles as received from the vendor. The ssDNA and gold nanoparticles were mixed by vortexing for 2 s and then allowed to sit at room temperature (21 °C) for 18 h. A concentrated 5.5 mol·L^{-1} NaCl solution was added to bring the total salt concentration to a first step of 0.11 mol·L^{-1}. The mixture was vortexed and allowed to sit at room temperature for 3 h before adding an additional volume of concentrated NaCl solution to raise the final NaCl concentration with the purpose of increasing the ssDNA loading on the particles. Final NaCl concentrations used for this study were 0.80, 1.52, and 2.41 mol·L^{-1} with ssDNA concentrations decreasing from 11 to 6 μmol·L^{-1} as the salt concentration increased. It was estimated that the concentration of the ssDNA in solution was a factor of 10 or greater in excess of the concentration needed to result in full monolayer coverage for gold nanoparticles assuming that saturation coverage is $\sim 2.5 \times 10^{13}$ strands·cm^{-2} as determined by Demers et al.[27] After the desired final salt concentration was achieved, the mixture was allowed to sit for 48 h at room temperature. The ssDNA-modified particles were then pelleted in their holding tubes using a Beckman Coulter (Fullerton, CA) Optima Max-XP benchtop ultracentrifuge outfitted with a MLS-50 swinging bucket rotor outfitted with Beckman Coulter Konical vials at a rotational speed of 2260 rad·s^{-1} (21 600 r·min^{-1}) for 15 min. All but 20 μL of the supernatant was withdrawn to leave a pellet of nanoparticles; the supernatant was replaced with an equal volume of deionized water and the ssDNA-gold particles were completely resuspended by vortexing for 2 s. The water suspending the particles was exchanged twice in total to decrease the NaCl concentration to approximately 0.01 mol·L^{-1}.

Dynamic Light Scattering. A Malvern Zetasizer Nano (Worcestershire, U.K.) was used to perform dynamic light scattering at a 3 rad (173 degree) backscattering angle for samples 100 μL in volume. For these experiments, samples of DNA-modified gold nanoparticles were recovered from the AUC cells and filtered through 4.5×10^{-7} m (0.45 μm) polyvinylidene fluoride membrane filters (Daigger, Vernon Hills, IL) to remove dust. The gold nanoparticles have a surface-plasmon resonance (SPR) with a

(15) Cölfen, H.; Völkel, A. *Prog. Colloid Polym. Sci.* **2004**, *127*, 31–47.
(16) Mayya, K. S.; Schoeler, B.; Caruso, F. *Adv. Funct. Mater.* **2003**, *13*, 183–188.
(17) Döllefeld, H.; McGinley, C.; Almousalami, S.; Möller, T.; Weller, H.; Eychmuller, A. *J. Chem. Phys.* **2002**, *117*, 8953–8958.
(18) Mächtle, W. *Biophys. J.* **1999**, *76*, 1080–1091.
(19) Calabretta, M. K.; Matthews, K. S.; Colvin, V. L. *Bioconjugate Chem.* **2006**, *17*, 1156–1161.
(20) Jamison, J. A.; Krueger, K. M.; Yavuz, C. T.; Mayo, J. T.; LeCrone, D.; Redden, J. J.; Colvin, V. L. *ACS Nano* **2008**, *2*, 311–319.
(21) Jamison, J. A. Colvin, V. L. *Abstracts of papers*, 232nd ACS National Meeting, San Francisco, CA; American Chemical Society: Washington DC, 2006; Abstract INOR-753.
(22) Calabretta, M. K.; Jamison, J. A.; Falkner, J. C.; Liu, Y.; Yuhas, B. D.; Matthews, K. S.; , V. L. *Nano Lett* **2005**, No.5, 963–7.
(23) Kaiser, D. L.; Watters, R. L. *Reference Material 8011 Gold Nanoparticles, Nominal 10 nm Diameter*. 2007, https://www-s.nist.gov/srmors/view_detail.cfm?srm=8011 (accessed April 2010).
(24) Kaiser, D. L.; Watters, R. L. *Reference Material 8012 Gold Nanoparticles, Nominal 30 nm Diameter*. 2007, https://www-s.nist.gov/srmors/view_detail.cfm?srm=8012 (accessed April 2010).
(25) Kaiser, D. L.; Watters, R. L. *Reference Material 8013 Gold Nanoparticles, Nominal 60 nm Diameter*. 2007, https://www-s.nist.gov/srmors/view_detail.cfm?srm=8013 (accessed April 2010).
(26) Pease, L. F.; Tsai, D.-H.; Zangmeister, R. A.; Zachariah, M. R.; Tarlov, M. J. *J. Phys. Chem. C* **2007**, *111*, 17155–17157.
(27) Demers, L. M.; Mirkin, C. A.; Mucic, R. C.; Reynolds, R. A.; Letsinger, R. L.; Elghanian, R.; Viswanadham, G. *Anal. Chem.* **2000**, *72*, 5535.

peak absorption wavelength of 520 nm. The 633 nm wavelength of the DLS probe laser is sufficiently far from the SPR absorption peak that the SPR does not perturb the DLS measurement.

Analytical Ultracentrifugation. Analytical ultracentrifugation of all samples was performed using a Beckman Coulter XL-A with a titanium 4 place rotor (Beckman Coulter). Cells were outfitted with quartz windows and Epon 12 mm path length dual sector centerpieces and quartz windows. The reference sector of each cell was filled with 425 μL of deionized water while the sample sector was filled with 400 μL of ssDNA modified or unmodified gold nanoparticles suspended in deionized water. Absorbance was measured at a wavelength of 520 nm at scan intervals of 0.007 cm. Gold nanoparticles (5 and 10) nm in diameter were centrifuged at 1570 rad$\cdot$s^{-1} (15 000 r$\cdot$min^{-1}) and 20 nm gold nanoparticles were centrifuged at 523 rad$\cdot$s^{-1} (5000 r$\cdot$min^{-1}). Bare gold nanoparticles 30 and 60 nm in diameter were centrifuged at 262 rad$\cdot$s^{-1} (2500 r$\cdot$min^{-1}). All AUC runs were performed at 20 °C. The samples were scanned at least 10 times at intervals of 130 s before the nanoparticles completely pelleted at the bottom of the cell. We determined that 10 scans were adequate by comparing the sedimentation coefficient distribution calculated from a 20-scan set of the system 10 nm gold coated with ssDNA 30-mers with the results from two 10-scan subsets created from the even and odd scans of the 20-scan set. Values of the c(s) fits of the sedimentation coefficients for the 20-scan subsets, as determined from Sedfit, agreed to within less than 1 Sv of each other and to within 1 Sv of the 20-scan set.

The concentration of a suspension may affect the sedimentation rate of the suspended particles. We confirmed that concentration effects were negligible in two ways. First, sedimentation velocity measurements were obtained from 10 and 20 nm bare gold nanoparticles at the as-supplied concentration and then diluted by a factor of 2 and a factor of 4. For each size nanoparticle, the weight average sedimentation coefficients obtained at the three different concentrations were equal to within the standard deviation observed for repeat measurements. Second, we calculated the effect of particle charge on the sedimentation coefficient, using accepted models of electroviscosity. The ratio of the sedimentation velocity of a charged sphere to that of an otherwise identical uncharged sphere is given as

$$\frac{u'_{St}}{u_{St}} = \frac{1}{1+\left(\frac{2m\sigma^2}{\rho_s \eta V k}\right)} \quad (1)$$

where u'_{st} is the Stokes sedimentation velocity of a charged particle, u_{st} is the Stokes sedimentation velocity of an uncharged particle, m is the total mass of particles added to volume V, σ is the charge per unit area on the surface of the sphere, ρ_s is the density of the particle, η is the viscosity of the liquid, and k is the ionic conductivity of the liquid. The model was applied to 10 and 20 nm gold nanoparticles coated with 30-base ssDNA to test the case where the charge−charge repulsions should be greatest. We calculated the surface charge using literature values[27] for the surface coverage of ssDNA on Au nanoparticles and making the conservative assumption that each nucleotide carried a single negative charge. Sedimentation velocity experiments were performed at 75% of their as-delivered concentration. The model shows that there is virtually no impact on the sedimentation velocity of the ssDNA-coated particles. The 10 nm gold particles covered with ssDNA 30-mers exhibited a Stokes velocity ratio of 0.99 and 20 nm gold particles covered with ssDNA 30-mers exhibited a Stokes velocity ratio of 0.98.

Results and Discussion

Biologically Modified Gold Particles. Raw sedimentation velocity data from multiple scans of a cell containing unmodified, citrate-stabilized 10 nm gold nanoparticles are displayed in Figure 1.

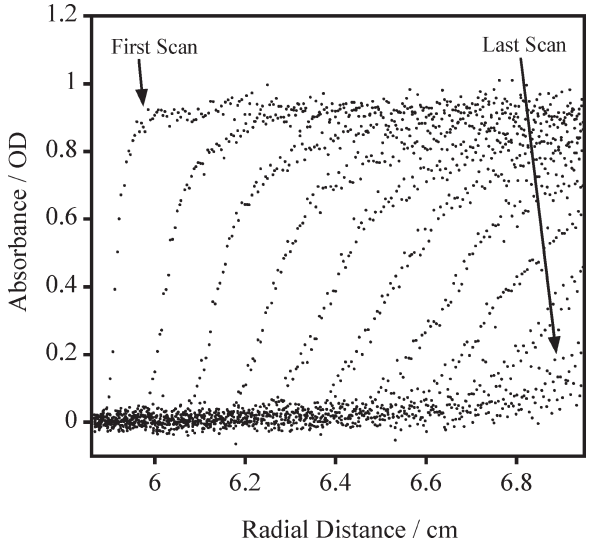

Figure 1. AUC scans for unmodified 10 nm diameter gold nanoparticles centrifuged 1570 rad$\cdot$s^{-1} (15 000 r$\cdot$min^{-1}). The position of each scan is measured in centimeters from the center of the rotor. Successive scans were taken 130 s apart.

These data are typical for all gold nanoparticle sample solutions examined in this study. Modification of gold nanoparticles with thymidine homo-oligonucleotides was selected for our studies because this system has been extensively studied on planar gold surfaces where it has been established that thymidine bases have a relatively low affinity for gold surfaces[28] and base-pairing interactions are weak.[29] These factors tend to favor relatively high surface coverages and an upright configuration for thiol-modified thymine strands attached to gold surfaces. This is in contrast to the adsorption behavior of adenine, cytosine and guanine homo-oligonucleotides on gold, which is significantly more complex due to strong base-gold surface interactions or base-pairing effects. Sedimentation of the 10 nm ssDNA covered gold nanoparticles was carried out in both pure water (residual NaCl concentration less than 0.01 mol$\cdot$L^{-1}) and 1 mol$\cdot$L^{-1} solutions of NaCl and $MgCl_2$.

Sedimentation coefficients were calculated from the raw data using Sedfit by Schuck.[30] The continuous c(s) model was used to fit the data with a f/f_0 factor of 1.2 for both bare and ssDNA coated 10 nm gold nanoparticles. The 20 nm gold particles were fit with f/f_0 varying from 0.98 to 1.45 for bare to SH-T30 coated 20 nm gold particles. Sedfit numerically fits the Lamm Equation to the complete set of 520 nm wavelength absorbance scans of each sample cell shown in Figure 1. Representative sedimentation coefficient distributions for bare 10 nm gold particles and 10 nm particles with increasingly longer ssDNA strands from 5 to 30 bases in length are displayed in Figure 2. These data have several noteworthy features. First, modification of nanoparticles with DNA reduces their sedimentation coefficient. Second, as the length of DNA increases, the sedimentation coefficient distribution moves monotonically to lower values. Weight average sedimentation coefficients were calculated using the integrate feature of Sedfit[30] and these values are plotted in Figure 3 for the 10 nm ssDNA modified particles as a function of ssDNA length in pure water and 1 mol$\cdot$L^{-1} NaCl and $MgCl_2$ solutions. We were unable

(28) Kimura-Suda, H.; Petrovykh, D. Y.; Tarlov, M. J.; Whitman, L. J. *J. Am. Chem. Soc.* **2003**, *125*, 9014–9015.
(29) Murphy, M. C.; Rasnik, I.; Cheng, W.; Lohman, T. M.; Ha, T. *Biophys. J.* **2004**, *86*, 2530–2537.
(30) Schuck, P. *Biophys. J.* **2000**, *78*, 1606–1619.

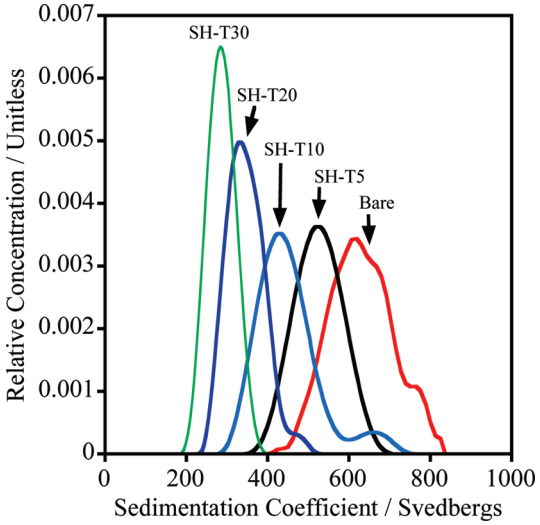

Figure 2. Progression of the sedimentation coefficient distribution for bare 10 nm gold particles and 10 nm gold particles modified with thymidine homo-oligomers 30 bases (SH-T30) to 5 bases (SH-T5).

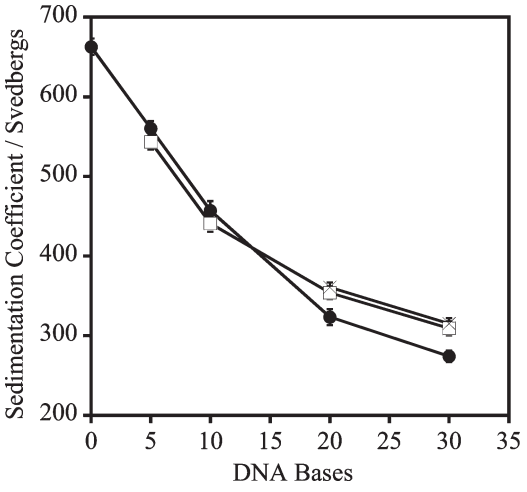

Figure 3. Sedimentation coefficients for 10 nm diameter gold nanoparticles with ssDNA of varying number of thymidine bases in (●) pure water, (□) 1.0 mol·L^{-1} aqueous NaCl solution, and (×) 1.0 mol·L^{-1} aqueous $MgCl_2$ solution. Error bars represent standard deviations.

to calculate a particle size distribution from the sedimentation coefficient distribution due to the fact that the as-received nanoparticles are too dilute at ~0.5 mg·mL^{-1} to determine their partial specific volume by the standard method of diluting the sample and measuring its density.

The sedimentation coefficients for the DNA-modified gold nanoparticles decreases monotonically with the number of thymidine, dT, nucleotides or strand length. We note that the reproducibility of the sedimentation coefficients is excellent as evidenced by the small standard deviations derived from 3 measurements of the same sample. Repeat sedimentation velocity experiments were performed by removing the cell and shaking it by hand to resuspend the nanoparticles. The sedimentation coefficients for 10 nm nanoparticles derivatized with thymidine 5- and 10-mers were not measured in 1 mol·L^{-1} $MgCl_2$ because significant flocculation occurred in these solutions. In addition, the sedimentation coefficients of gold nanoparticles with thymidine 20- and 30-mers in pure water appear to be slightly lower than those

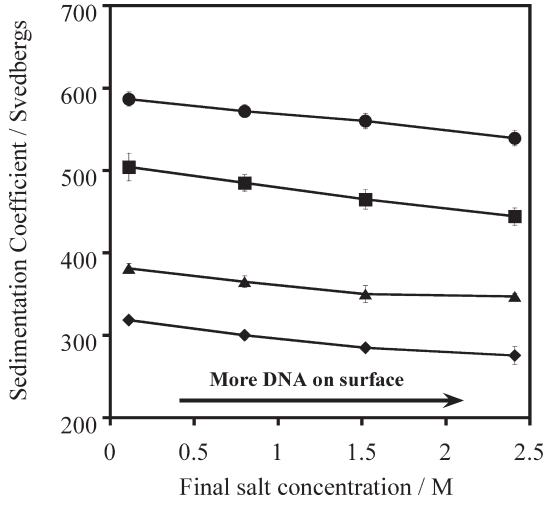

Figure 4. 10 nm gold nanoparticles modified with thiolated SH-T5 (●), SH-T10 (■), SH-T20 (▲), and SH-T30 (♦) sedimented in pure water. Error bars represent standard deviations.

sedimented in 1 mol·L^{-1} salt solution suggesting that the apparent density of the ssDNA modified nanoparticles is higher in salt solution. The density and viscosity of 1 mol·L^{-1} NaCl and $MgCl_2$ solutions were entered into Sedfit to place the sedimentation coefficients on the same basis as the sedimentation coefficients in pure water. Our prior calculation for the effect of charge−charge repulsions shows that the higher sedimentation coefficients for ssDNA coated nanoparticles in 1 mol·L^{-1} are not caused by charge screening in the presence of salt ions. This suggests that the DNA strands on the particle's surface assume a more compact configuration consistent with the persistence length of the ssDNA strands decreasing with salt concentration.[29] The sedimentation coefficients of ssDNA gold particles centrifuged with either dissolved Mg^{2+} or Na^+ ions were identical.

Detecting Differences in ssDNA Surface Coverage with AUC. We also found that AUC can detect differences in surface coverage of ssDNA homo-oligomers on gold nanoparticles. Analytical ultracentrifugation has been able to distinguish subnanometer size differences in solid particles.[31,32] To vary the surface coverage of ssDNA on gold nanoparticles, different batches of thymidine-modified 10 nm gold nanoparticles were prepared with systematically higher ending NaCl concentrations to progressively increase the surface loading of ssDNA. In these experiments, all samples were resuspended in pure deionized water before sedimentation in the AUC. Figure 4 demonstrates that an increase in ssDNA surface coverage (more salt added during the attachment phase to promote more ssDNA attachment on the gold nanoparticle)[33] leads to a slight, but significant,[34] decrease in the weight average sedimentation coefficient. Coating of a Au nanoparticle by ssDNA increases the hydrodynamic radius and reduces the average density of the particle; the net result is a reduction in the sedimentation coefficient. The density reduction is muted when ssDNA is added to nanoparticles with larger diameters due to the significant decrease in surface area to volume ratio.

Particle Models. Two models were developed to provide greater insight into the experimental trends in sedimentation coefficients as a function of the length of the ssDNA. The first

(31) Cölfen, H.; Pauck, T. *Colloid Polym. Sci.* **1997**, *275*, 175–180.
(32) Cölfen, H. *ACS Symp. Ser.* **2004**, *881*, 119–137.
(33) Petrovykh, D. Y.; Kimura-Suda, H.; Whitman, L. J.; Tarlov, M. J. *J. Am. Chem. Soc.* **2003**, *125*, 5219–5226.
(34) Veronese, F. M. *Biomaterials* **2001**, *22*, 405–417.

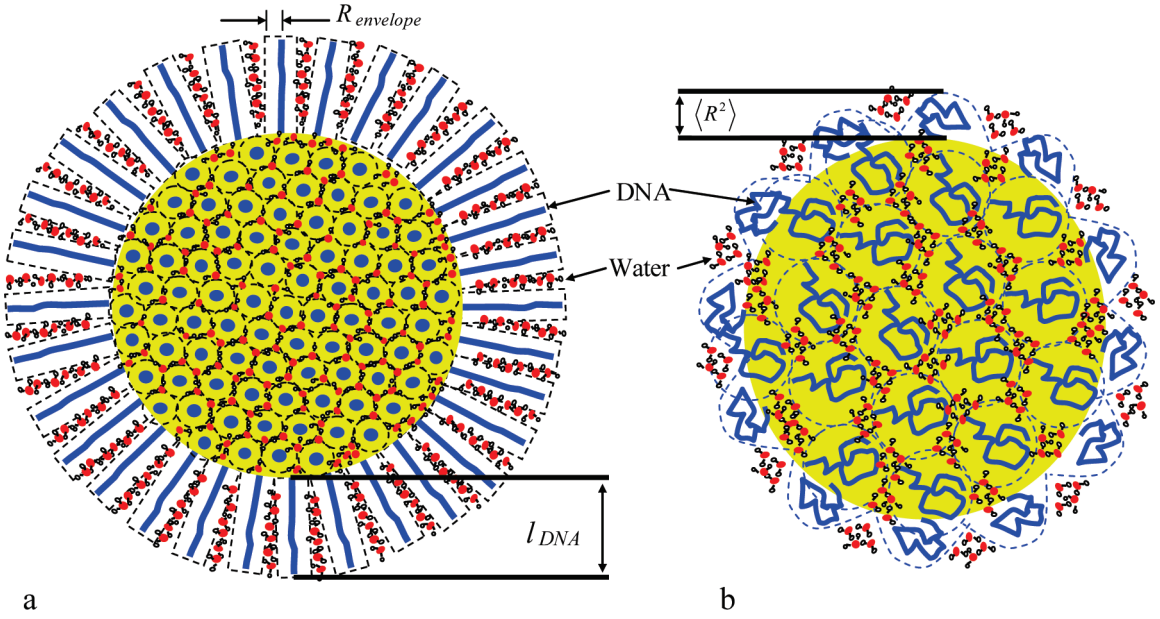

Figure 5. Particle models (a) hydrated fully extended chain (FEC) and (b) hydrated worm like chain (WLC).

model illustrated in Figure 5a treats the derivatized particle as having fully extended chain (FEC) dT strands tethered to the particles in a hexagonal close packed formation. Although it is unlikely that the ssDNA strands are hexagonally close packed on the nanoparticle surface, we believe this assumption is reasonable because only a weak dependence of ssDNA coverage on the sedimentation coefficient is observed in Figure 3. The second model illustrated in Figure 5b treats each dT strand as a worm like chain (WLC) that is coiled randomly about its thiol tether. The overall density of the bare or ssDNA-modified particle is calculated by the general relationship

$$\rho_2 = \frac{M_{DNA} + M_p + M_w}{V_{DNA} + V_{particle} + V_w} \quad (2)$$

where ρ_2 is the density of the bare or ssDNA modified particle, M_{DNA} is the total mass of ssDNA attached to the particle, M_p is the mass of the gold particle, and M_w is the mass of the water hydrating the chains of ssDNA. The total volume of the particle consists of the sum of the volumes of the gold particle ($V_{particle}$), the ssDNA molecules (V_{DNA}), and the water confined between ssDNA chains (V_w).

The FEC ssDNA model is illustrated in Figure 5a with water of hydration filling the space between the ssDNA chains. Each chain of ssDNA extends normal to the surface and a dry cylindrical envelope surrounding the chain is used to prevent the model from placing water in the same space as the ssDNA chain. The relationship for calculating the overall density of a bare or ssDNA modified gold nanoparticle with the FEC assumption is as follows:

$$\rho_2 = \frac{m_{DNA} n_{DNA}}{4/3\pi(r_p + l_{DNA})^3} + \frac{\rho_p {r_p}^3 + \rho_w (r_p + l_{DNA})^3 - \rho_w {r_p}^3}{(r_p + l_{DNA})^3} - \frac{n_{DNA}\rho_w l_{DNA} {r_{envelope}}^2}{1/3(r_p + l_{DNA})^3} \quad (3)$$

where m_{DNA} is the mass of one ssDNA chain, n_{DNA} is the number of ssDNA chains on one gold nanoparticle, l_{DNA} is the length of one DNA chain, ρ_p is the density of the gold nanoparticle, r_p is the radius of the gold nanoparticle, $r_{envelope}$ is the radius of a dry cylindrical envelope surrounding the fully extended chain, and ρ_w is the density of liquid water between chains of ssDNA. The length of the fully extended ssDNA and the volume of the dry envelope around each chain are calculated using an individual dT length of 0.59 nm.[26] This model was used to predict only sedimentation coefficients in pure water therefore the density of the water between ssDNA molecules was assumed to be the density of bulk water at 20 °C or 998.23 $kg \cdot m^{-3}$. While the density of water confined between ssDNA molecules may be different from bulk water, the difference is likely insignificant to the numerical result. The density of gold nanoparticles is assumed to be that of bulk gold (19 300 $kg \cdot m^{-3}$) based on the finding of Li et al.[35] that gold clusters as small as 20 atoms have the same atomic packing as bulk gold. For these calculations, we consider the ssDNA adsorbed on the surface of the nanoparticles to be hexagonally close packed. We note again that this assumption is a simplification and it is unlikely that adsorbed chains possess any long-range order on the nanoparticle surface.

With the density of the modified gold nanoparticle calculated by the model, the sedimentation coefficients of the biologically modified gold particle are calculated with an expression based on the Svedberg relationship. The suspension of particles was treated as a dilute system with no particle interactions leading to the following relationship for the sedimentation coefficient, s. The full derivation was provided in the Supporting Information:

$$s = \frac{2{R_s}^2(\rho_2 - \rho_1)}{9\eta_1} \quad (4)$$

where ρ_1 is the matrix fluid density, ρ_2 is the density of the hydrated ssDNA-modified nanoparticle, η_1 is the viscosity of the matrix fluid, and R_s is the radius of a spherical nanoparticle.

Figure 6 shows a comparison of FEC model predictions (dashed lines) with experimentally determined sedimentation coefficients. The FEC model predictions using the bulk density of gold

(35) Li, J.; Li, X.; Zhai, H.-J.; Wang, L.-S. *Science* **2003**, *299*, 864–867.

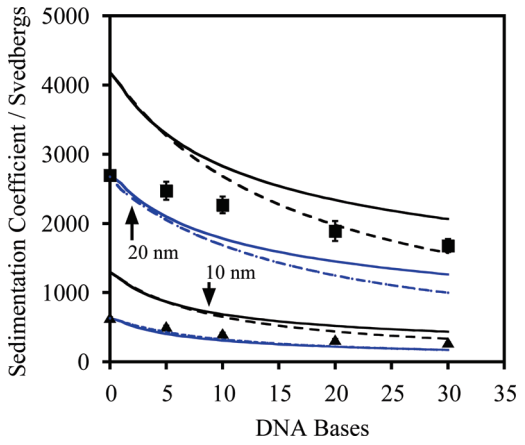

Figure 6. Comparison of (—) WLC and (– –) FEC models with measured sedimentation coefficients for (▲) 10 nm and (■) 20 nm diameter gold nanoparticles derivatized with thymidine homo-oligomers. All sedimentation velocity experiments were performed in pure water. The models represented by the black lines employ the density of bulk gold, 19 300 kg·m^{-3}. Models represented by the blue lines employ the average density predicted by DLS measurements of bare gold nanoparticles: 9 900 kg·m^{-3} for modified 10 nm nanoparticles and 12 800 kg·m^{-3} for modified 20 nm nanoparticles. Error bars represent standard deviations.

(19 300 kg·m^{-3}) had an absolute average deviation (AAD) from the measured sedimentation coefficients of ~60% for 10 nm gold nanoparticles and ~25% for 20 nm gold nanoparticles. When the apparent density of gold was used the FEC model produced an AAD of ~21% for 10 nm gold nanoparticles and ~23% for 20 nm gold nanoparticles. When the apparent density of gold was used the model falls below all of the 20 nm sedimentation coefficients, however, using the bulk density of gold, reasonable agreement between the measured sedimentation coefficients and the FEC predictions is found for 20 nm gold nanoparticles modified with 20 and 30 dT chains.

Wormlike Chain Model. Since ssDNA chains more likely adopt a random coil configuration, the wormlike chain (WLC) model[36] was used to calculate the radius of the hemispherical ssDNA coils on the surface of the gold particle. A particle representing the WLC model is illustrated in Figure 5b. Each end-tethered ssDNA molecule is confined to a dry hemispherical envelope to prevent water from occupying the same space as the ssDNA and the envelopes are again assumed to arrange in hexagonal close packing on the gold surface. The WLC model for polymer chains is selected because it has been previously used to model the end-to-end distance of single and double stranded DNA.[29] The WLC model for polymer chains requires just two parameters: the fully extended length of the ssDNA chain and the persistence length to model the stiffness of the molecule. These two parameters are related as

$$\langle R^2 \rangle = 2l_p R_{max} - 2{l_p}^2 \left(1 - \exp\left(\frac{R_{max}}{l_p}\right)\right) \quad (5)$$

where $\langle R^2 \rangle$ is the end-to-end distance of the ssDNA chain, R_{max} is the length of a fully extended ssDNA chain, and l_p is the persistence length of a ssDNA chain. Values of R_{max} and l_p for both the (10 and 20) nm ssDNA modified gold nanoparticles are contained in Table 1. A value of 2.5 nm is used for the persistence length of thymine homo-oligomers in pure water as reported by Murphy et al.[29] The R_{max} varied from approximately 3 to 18 nm based on a 0.59 nm length for each base.[26] The relationship for the overall density of bare or ssDNA modified gold nanoparticles is as follows:

$$\rho_2 = \frac{m_{DNA} n_{DNA}}{4/3\pi(r_p + \langle R^2 \rangle)^3} + \frac{\rho_p {r_p}^3 + \rho_w (r_p + \langle R^2 \rangle)^3 - \rho_w {r_p}^3 - n_{DNA}\rho_w \langle R^2 \rangle^3/2}{(r_p + \langle R^2 \rangle)^3} \quad (6)$$

Predictions of measured sedimentation coefficients by the WLC model assuming a gold core density (ρ_p) of 19 300 kg·m^{-3} are shown as the solid lines in Figure 6. The WLC model sedimentation coefficient predictions are higher than those of the FEC model because the sphere encompassing the worm-like ssDNA layer has a smaller diameter than the layer of fully extended ssDNA and hence the average density of the gold and ssDNA shell is lower when the ssDNA shell is thicker. As a result, the WLC model (with a gold density of 19 300 kg·m^{-3}) provides poorer agreement than the FEC model (with a gold density of 19 300 kg·m^{-3}), most notably at longer strand lengths, with absolute average deviations (AAD) of ~70% for 10 nm gold nanoparticles and ~30% for 20 nm gold nanoparticles. When the apparent density of 10 nm gold particles was used the AAD was ~16% for 10 nm gold particles and the AAD was ~17% for 20 nm gold particles. Dynamic light scattering was performed

Table 1. Parameters of eq 5

nominal particle size/nm	# bases per homo-oligomer	R_{max}/ nm	l_p/nm
10	5	2.95	2.5
10	10	5.90	2.5
10	20	18.8	2.5
10	30	17.7	2.5
20	5	2.95	2.5
20	10	5.90	2.5
20	20	18.8	2.5
20	30	17.7	2.5

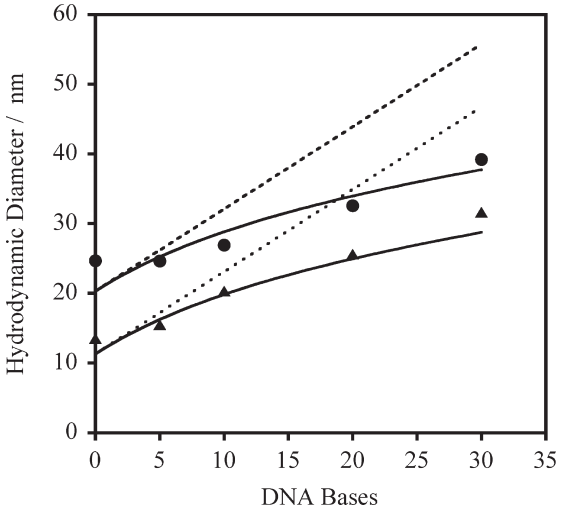

Figure 7. Hydrodynamic diameters measured by dynamic light scattering for thymidine modified (▲) 10 nm gold nanoparticles and (●) 20 nm gold nanoparticles as predicted by the (—) WLC model and (– –) FEC model.

(36) Rubenstein, M.; Colby, R. H. *Polymer Physics*; Oxford University Press: New York, 2003.

Table 2. Bare Particle Sizes

nominal particle size/nm	measured particle size/nm	references
5	8.45	
10	11.3[a]	23
20	20.3	
30	28.4[a]	24
60	56.3[a]	25

[a] ES-DMA measurement only.

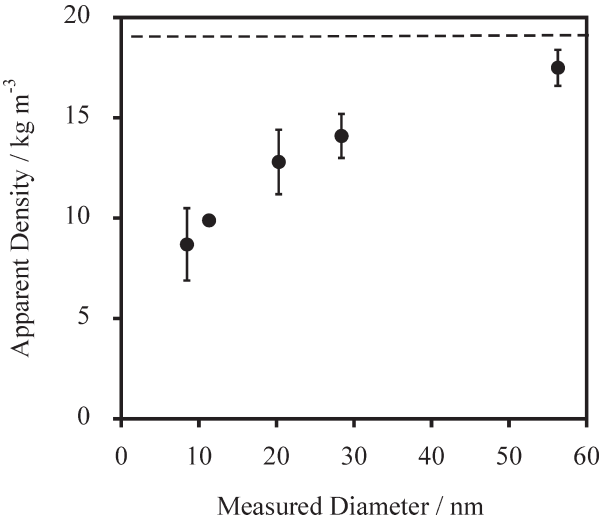

Figure 8. Bare citrate stabilized gold particles sedimented in deionized water. The dashed line marks the density of bulk gold 19 300 $kg \cdot m^{-3}$. Error bars represent standard deviation.

to determine whether the WLC or FEC model predicted the diameter of the particles more accurately. Figure 7 plots the measured hydrodynamic diameter of bare and ssDNA modified gold nanoparticles in pure water along with diameter predictions from both the WLC and FEC models. The FEC model overestimates the measured hydrodynamic diameters for strands greater than 5 bases in length, whereas the WLC model predictions follow the measured diameters more closely. Thus, the poorer sedimentation coefficient predictions by the WLC model shown in Figure 6 are most likely due to the predicted particle density being higher than the apparent particle density because the friction factors should be similar for all the spherical ssDNA modified particles. The overprediction of the measured sedimentation coefficients could be caused by a hydration layer extending beyond the envelopes surrounding the ssDNA shown in Figure 5. An expanded hydration layer was not detected by DLS and the diameters for ssDNA modified gold particles predicted by the WLC model for ssDNA modified gold nanoparticles matched the DLS measured diameters.

To illustrate the degree to which the apparent density of bare gold nanoparticles varies with the particle diameter in pure water, sedimentation velocity experiments were performed on bare gold nanoparticles with nominal diameters from 5 to 60 nm listed in Table 2. Equation 4 was used to calculate the apparent density of the bare particles, ρ_2, from the measured sedimentation coefficient and measured particle diameter as determined with electrospray differential ion mobility analysis (ES-DMA).[26] Figure 8, which plots the apparent particle density from AUC versus the measured particle diameter, demonstrates that the hydration of the gold nanoparticle significantly lowers the calculated density of bare gold nanoparticles. The thickness of the hydration layer corresponding to the densities reported in Figure 8 varies from 1.5 to 1.59 nm, corresponding to a hydrodynamic diameter 3.0−3.18 nm larger than the diameter measured by ES-DMA. Inspection of the DLS results in Figure 7 for bare gold particles show that the measured hydrodynamic diameter of bare gold particles exceeds the ES-DMA values by approximately this amount. Nanoparticles in the range of 60 nm and above appear to obey the Svedberg equation and their apparent density approaches that of bulk gold (19 300 $kg \cdot m^{-3}$). This hydration effect for gold nanoparticles below 60 nm may also affect the gold nanoparticles with the shortest length ssDNA homo-oligomers if the ssDNA cannot completely block water molecules from interacting with the gold surface. A series of ssDNA coated gold nanoparticles ranging from 5 to 60 nm was not created because we were not able to modify the 30 or 60 nm gold particles with ssDNA due to flocculation of particles upon addition of 5 $mol \cdot L^{-1}$ NaCl solution.

The blue lines in Figure 6 show the WLC and FEC models with the bulk density of gold replaced by the apparent density from Figure 8. The resulting models give sedimentation coefficients that are below the measured sedimentation coefficients with only the sedimentation coefficient of the bare gold nanoparticle being predicted accurately. An additional factor is necessary to tune the apparent density so that the model predicted sedimentation coefficients in Figure 6 decline less steeply as the ssDNA length decreases. We conjecture that the addition of a full hydration shell to obtain the hydrodynamic diameter overestimates the degree of hydration for the longer ssDNA oligomers; in effect the WLC and FEC models already account for significant hydration of the ssDNA.

Conclusions

This paper demonstrates that changes in the length of thymidine oligonucleotides immobilized on nanoparticle surfaces can be detected by analytical ultracentrifugation along with differences in molecular surface loading. Prediction of the sedimentation coefficients from models for bare and ssDNA modified gold nanoparticles was not entirely possible due to the hydration effects that reduce the nanoparticle's density below that of bulk gold in an aqueous medium. The hydrodynamic diameters of unmodified and ssDNA modified gold nanoparticles measured with DLS were matched well by the WLC model using the same parameters. This revealed that the WLC model will determine a plausible overall diameter for the ssDNA modified gold nanoparticle and the reason for the WLC model's poor sedimentation coefficient prediction may be due to the presence of hydration layer effects. This layer of hydration was found to be significant for gold nanoparticles below 60 nm in diameter. In contrast, the apparent density of gold nanoparticles 60 nm and higher approaches that of bulk gold (19 300 $kg\ m^{-3}$). The difference between the sedimentation coefficient predictions of the WLC and FEC models and the measured sedimentation coefficients increases as the ssDNA chain length is reduced. Future modeling should focus on the effect of hydration to adequately predict the sedimentation coefficient of biologically modified gold nanoparticles. Overall, the precision of AUC makes it a well-suited analytical method to perform quality control tests of biologically modified nanomaterials at various stages in their processing.

Acknowledgment. We thank Edward Eisenstein of the Center for Advanced Research in Biotechnology for allowing us access to the AUC. We thank Walter Stafford and David Hayes of the Boston Biomedical Research Institute for advice on AUC technique, raw data analysis, and modeling the sedimentation coefficient of nanomaterials. We thank Jack

Douglas of the NIST Polymer Division for advice on the modeling of ssDNA covered nanoparticles. We thank Patrick Brown and Peter Schuck of the National Institutes of Health for advice on the analysis of raw data. We thank Suvajyoti Guha for measuring the diameters of two sizes of bare gold nanoparticles with ES-DMA and Professor Michael Zachariah for the use of his ES-DMA instrument. We also thank Germarie Sánchez-Pomales and Joshua Wayment for their help in the final stage of this project. J.B.F. thanks the National Research Council for his postdoctoral research fellowship.

Supporting Information Available: Full equation derivation and additional figures. This material is available free of charge via the Internet at http://pubs.acs.org.